TORUS MODELS OF ACTIVE GALACTIC NUCLEI IN THE LOCAL UNIVERSE (Galaxy 29b)

Kohei Ichikawa[1]

[1] Department of Astronomy, Graduate School of Science, Kyoto University, Kitashirakawa-Oiwake cho, Kyoto 606-8502, Japan

E-mail: ichikawa@kusastro.kyoto-u.ac.jp

ABSTRACT

We investigate the mid- (MIR) to far-infrared (FIR) properties of a nearly complete sample of local active galactic nuclei (AGNs) detected in the *Swift*/Burst Alert telescope (BAT) all-sky hard X-ray (14–195 keV) survey, based on the cross correlation with the *AKARI* infrared survey catalogs complemented by those with *IRAS* and *WISE*. Out of 135 non-blazar AGNs in the *Swift*/BAT 9-month catalog, we obtain the MIR photometric data for 128 sources in either the 9, 12, 18, 22, or 25 μm band. We find a good correlation between their hard X-ray and MIR luminosities over three orders of magnitude ($42 < \log \lambda L_{\lambda}(9, 18\ \mu\mathrm{m}) < 45$), which is tighter than that with the FIR luminosities at 90 μm. Both X-ray unabsorbed and absorbed AGNs follow the same correlation, implying isotropic infrared emission, as expected in clumpy dust tori rather than homogeneous ones.

key words: galaxies: active — galaxies: nuclei — infrared: galaxies infrared - telescope: conferences - proceedings

1. INTRODUCTION

A complete survey of active galactic nuclei (AGNs) throughout the history of the universe is one of the main goals in modern astronomy, which is necessary to understand the evolution of supermassive black holes (SMBHs) in galactic centers and their host galaxies. Given the fact that the majority of AGNs are expected to be obscured by dust and gas surrounding the SMBH, observations in hard X-ray and mid-infrared (MIR) bands are proposed to be promising tools for detecting the whole populations of AGNs (both radio-quiet and loud ones) thanks to their stronger penetrating power than optical/UV lights and soft X-rays. To understand the efficiency and completeness of these two (hard X-ray and MIR) surveys, it is quite important to establish the relation between hard X-rays and infrared emission of AGNs based on a large sample of nearby, bright AGNs for which detailed studies can be made.

The *Swift*/Burst Alert Telescope (BAT) survey (Tueller et al. 2008) is one of the most sensitive all sky surveys in the hard X-ray band (>10 keV), providing us with the least biased sample of AGNs in the local universe, including heavily obscured ones. *Suzaku* follow-up observations of BAT AGNs have discovered a new type of deeply buried AGNs with a very small scattering fraction (Ueda et al. 2007). Assuming that the amount of gas responsible for scattering is not much different from other objects, it is suggested that these new type AGNs are obscured by a geometrically thick torus with a small opening angle. Understanding the nature of this population is important to reveal their roles in the cosmological evolution of SMBHs and host galaxies.

The MIR band also provides crucial information on the AGN tori. Many studies suggest that MIR emission is a good indicator of AGN activity. Gandhi et al. (2009) have found a strong correlation between X-ray (2–10 keV) and MIR (12.3 μm) luminosity from the nucleus of Seyfert galaxies, using Very Large Telescope/VISIR data where in many cases the AGN can be spatially resolved from the host galaxy.

We statistically examine the correlation between the infrared and X-ray luminosities of AGNs by utilizing a large uniform sample in the local universe, and investigate their infrared properties as a function of obscuration type. For this purpose, we use the *Swift*/BAT 9-month catalog (Tueller et al. 2008) as the parent sample, whose multiwavelength properties have been intensively investigated. Here we focus only on "non-blazar" AGNs. As for the infrared data, we primarily

use the all-sky survey catalogs obtained with *AKARI* (Murakami et al. 2007), which provide unbiased galaxy samples selected in the mid- and far-infrared (FIR) bands with unprecedented sensitivities as an all sky survey mission. To complement the infrared data of AGNs whose counterparts are not detected or do not have reliable flux measurements by *AKARI*, we also utilize the all sky survey catalog of NASA's *Wide-field Infrared Survey Explorer* (*WISE;* Wright et al. 2010) mission, as well as the catalogs of the *Infrared Astronomical Satellite* (*IRAS;* Neugebauer et al. 1984). Throughout the paper, we adopt $H_0 = 70.0$ km s^{-1} Mpc^{-1}, $\Omega_{\rm M} = 0.3$, and $\Omega_\Lambda = 0.7$. This paper gives a digest of Ichikawa et al. (2012), to which the reader is referred for details.

2. Sample Selection

2.1. Parent Sample and IR Counterparts

The *Swift*/BAT 9-month catalog (Tueller et al. 2008) contains 137 non-blazar AGNs with a flux limit of 2×10^{-11} erg cm^{-2} s^{-1} in the 14–195 keV band. The redshift range of this sample is $0 < z < 0.156$. Winter et al. (2009) investigated the soft X-ray (0.5–10 keV) properties of 128 (94.8%) BAT-detected non-blazar AGNs of Tueller et al. (2008). By fitting the X-ray spectra, they derive key spectral parameters, such as the absorption column density ($N_{\rm H}$), covering fraction of the absorber ($f_{\rm c}$) or the scattering fraction ($f_{\rm scat}$) with respect to the transmitted component ($f_{\rm scat} \simeq 1 - f_{\rm c}$). In our paper, we do not use the interacting galaxies NGC 6921 and MCG +04-48-002, which are not separated in the *Swift*/BAT catalog. Hence, the parent sample consists of 135 sources.

We determine the IR counterparts of the *Swift*/BAT AGNs by cross-correlating the *AKARI*, *IRAS*, and *WISE* catalogs in this order. Out of the 135 *Swift*/BAT AGNs, we identify total 128 MIR counterparts detected any in the 9, 12, 18, 22, or 25 μm. Thus, the completeness of detection in the MIR band is 95%. We also correct *IRAS* 12/25 μm and *WISE* 12/22 μm luminosities into *AKARI* 9/18 μm ones. See the Section 2 in Ichikawa et al. (2012) for the details of the cross matching of the IR counterparts.

2.2. AGN Type

To examine the infrared properties for different AGN populations, we divide the sample into three types based on their X-ray spectra. The first one is "X-ray type-1" (hereafter type-1) AGNs, defined as those showing absorption column density of $N_{\rm H} < 10^{22}$ cm^{-2}. The second is "X-ray type-2" (hereafter type-2) AGNs that have $N_{\rm H} > 10^{22}$ cm^{-2}. In addition, we are interested in whether or not there is distinction in the IR properties of "new type" AGNs, which exhibit extremely small $f_{\rm scat}$, suggesting the geometrically thick tori around the nuclei. Here we define new type AGNs as those satisfying $f_{\rm scat} < 0.005$, which are treated separately from the other (normal) type-2 AGNs in this paper.

3. Result

Figure 1 shows the luminosity correlations in the luminosity range from 10^{41} erg s^{-1} to 10^{46} erg s^{-1} between the infrared (9, 18, or 90 μm) and *Swift*/BAT hard X-ray bands. Type-1, type-2, and new type AGNs are marked with squares (blue), circles (brown), and pentagons (violet), respectively. The small-filled symbols denote the data from *AKARI*, large-filled ones those from *IRAS*, and small-open ones those from *WISE*. In the figure, NGC 4395 is not shown due to its low luminosities $(\log \lambda L_\lambda(9\ \mu{\rm m}), \log \lambda L_\lambda(18\ \mu{\rm m}), \log L_{\rm HX}) = (39.98, 40.28, 40.81)$. As noticed from the figure, the MIR (both 9 and 18 μm) luminosities correlate well with hard X-ray luminosity over 3 orders of magnitude (from 10^{42}– 10^{45} erg s^{-1}). In the FIR (90 μm) band, by contrast, the correlation is much weaker with larger dispersion compared to the MIR bands, even though here we only plot AGNs detected at 90 μm with *AKARI*.

Least-square fits to the hard X-ray versus MIR luminosity plots with a power law model (i.e., a linear function for the logarithmic luminosities with the form of $\log(L_{\rm HX}/10^{43}) = a + b \log(\lambda L_\lambda(9, 18\ \mu{\rm m})/10^{43})$ give the following best-fit correlations:

$$\log \frac{L_{\rm HX}}{10^{43}} = (0.06 \pm 0.07) + (1.12 \pm 0.08) \log \frac{\lambda L_\lambda(9\ \mu{\rm m})}{10^{43}} \quad (1)$$

$$\log \frac{L_{\rm HX}}{10^{43}} = (0.02 \pm 0.07) + (1.10 \pm 0.07) \log \frac{\lambda L_\lambda(18\ \mu{\rm m})}{10^{43}} \quad (2)$$

To check the significance of the correlations between the hard X-ray and MIR/FIR luminosities (or fluxes), we perform Spearman's tests for the summed sample consisting of all AGN types. The results are summarized in Table 1. We find that both luminosity–luminosity and flux–flux correlations between the hard

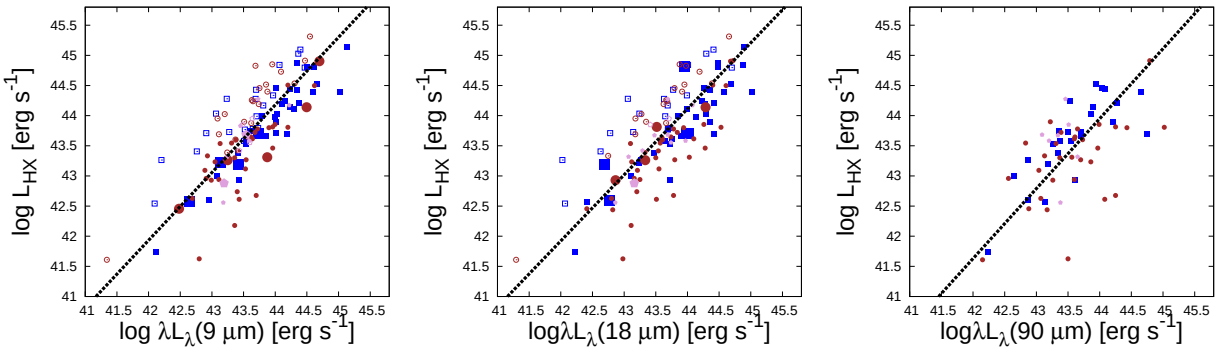

Figure 1: Correlation between infrared (9 μm, 18 μm, and 90 μm) and hard X-ray (14–195 keV) luminosities. Squares (blue) represent type-1 AGNs ($N_{\rm H} < 10^{22}$ cm^{-2}), circles (brown) type-2 AGNs ($N_{\rm H} \geq 10^{22}$ cm^{-2}), and pentagons (violet) new type AGNs ($f_{\rm scat} < 0.005$). Dotted lines represent the regression lines (see Section 3). The small-filled, large-filled, small-open symbols denote hard X-ray sources with the *AKARI*, *IRAS*, and *WISE* counterparts, respectively. The *IRAS* and *WISE* fluxes are all converted into the 9 μm or 18 μm band using the formula given in the Section 2.5 in Ichikawa et al. (2012).

Table 1.
Correlation Parameters between MIR and Hard X-Ray Sample

Sample	N	ρ_L	ρ_f	P_L	P_f	a	b
(1)	(2)	(3)	(4)	(5)	(6)	(7)	(8)
9 μm	126	0.82	0.60	3.0×10^{-31}	1.4×10^{-13}	0.06 ± 0.07	1.12 ± 0.08
18 μm	127	0.76	0.59	1.7×10^{-25}	2.4×10^{-13}	0.02 ± 0.07	1.10 ± 0.07
90 μm	62	0.59	0.17	4.5×10^{-7}	1.8×10^{-1}	-0.21 ± 0.10	1.16 ± 0.11

Table 1: Correlation proporties between 14-195 keV X-ray luminosity ($\log L_{\rm HX}$) and infrared (9, 18, and 90 μm) luminosities ($\log \lambda L_\lambda(9, 18, 90\ \mu{\rm m})$) to various subsample populations. (1) sample name; (2) number of sample; (3) the Spearman's Rank coefficient for luminosity correlations (ρ_L) ; (4) the Spearman's Rank coefficient for flux-flux correlations (ρ_f); (5) the standard Student t-test null significance level for luminosity correlations (P_L); (6) the standard Student t-test null significance level for flux-flux correlations (P_f); (7) regression intercept (a) and its 1σ uncertainty; (8) slope value (b) and its 1σ uncertainty. Equation is represented as $Y = a + bX$.

X-ray and MIR bands are highly significant. While there is also a significant correlation between 90 μm and hard X-ray luminosity, $(\rho_L, P_L) = (0.59, 4.5 \times 10^{-7})$, their flux–flux correlation is weak with $(\rho_f, P_f) = (0.17, 0.18)$.

We establish a tight correlation between the MIR and hard X-ray luminosities in AGNs using so far the largest, uniform AGN sample in the local universe. The MIR emission from galaxies hosting an AGN is believed to originate mainly from high temperature ($\sim$ 150–300 K) dust emission heated by X-ray/UV photons from the central engine. Thus, if extinction is not important, the MIR luminosity is expected to be correlated with the intrinsic X-ray luminosity, the most reliable tracers of the AGN power (since our sample contains mostly Compton thin AGNs with $N_{\rm H} < 10^{24}$ cm^{-2}, the observed 14–195 keV luminosity can be regarded as the intrinsic one without any correction). On the other hand, the FIR emission comes both from cooler ($\sim$ 30 K) interstellar dust heated by stars in host galaxies and from the cooler (outer) part of the torus in the AGN. The contribution from the host galaxy increases the scatter of the observed luminosity correlation, depending on the total star forming rate over the whole galaxy. Our results demonstrate that the MIR emission is more suitable for estimating the AGN intrinsic power than the emission in the FIR band.

As noticed from Figure 1, all types of AGNs (type-1, type-2, and new type) seem to follow almost the same MIR versus hard X-ray luminosity correlation. To check this further, we plot $\lambda L_\lambda(9\ \mu{\rm m})/L_{\rm HX}$ and $\lambda L_\lambda(18\ \mu{\rm m})/L_{\rm HX}$ as a function of the absorption column density ($N_{\rm H}$) in Figure 2. In both panels, there is no clear dependence of the MIR to hard X-ray luminosity ratio on $N_{\rm H}$ up to $\log N_{\rm H} \simeq 24$. The large ratios found for Compton thick AGNs can be partially explained by attenuation of the hard X-ray fluxes due to heavy obscuration. The absence of $N_{\rm H}$ dependence suggests that the emission from the AGN-heated dust seems not to be affected by the obscuration by the

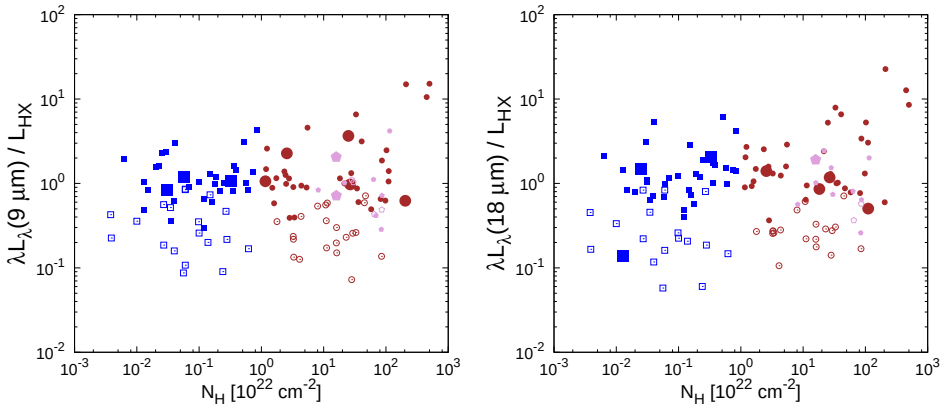

Figure 2: The MIR to hard X-ray luminosity ratio plotted against the absorption column density. Left: $\lambda L_\lambda(9\ \mu\mathrm{m})/L_{\mathrm{HX}}$. Right:$\lambda L_\lambda(18\ \mu\mathrm{m})/L_{\mathrm{HX}}$. All symbols are the same as Figure 1.

torus causing the X-ray absorption. The results cannot be explained with homogeneous dust torus models (Pier & Krolik 1993), which predict the significant decrease in the MIR to X-ray luminosity ratio when an optically-thick line-of-sight through the torus primarily show cooler smooth-dust and a lower mid-infrared luminosity for the same X-ray luminosity than does an optically-thin one. Our results rather favor the clumpy dust tori (Nenkova et al. 2008), which predicts isotropic MIR emission, as discussed in Gandhi et al. (2009).

REFERENCES

Gandhi, P., et al., 2009, Resolving the mid-infrared cores of local Seyferts, A&A, 502, 457
Ichikawa, K., et al., 2012, Mid- and Far-infrared Properties of a Complete Sample of Local Active Galactic Nuclei, ApJ, 754, 45
Murakami, H., et al., 2007, The Infrared Astronomical Mission AKARI, PASJ, 59, 369
Nenkova, M., et al, 2008, AGN Dusty Tori. II. Observational Implications of Clumpiness, ApJ, 685, 160
Neugebauer, G., et al., The Infrared Astronomical Satellite (IRAS) mission1984, ApJL, 278, L1
Pier, E. A., & Krolik, J. H. 1993, Infrared Spectra of Obscuring Dust Tori around Active Galactic Nuclei. II. Comparison with Observations, ApJ, 418, 673
Tueller, J., et al., 2008, Swift BAT Survey of AGNs, ApJ, 681, 11
Ueda, Y., et al., 2007, Suzaku Observations of Active Galactic Nuclei Detected in the Swift BAT Survey: Discovery of a "New Type" of Buried Supermassive Black Holes, ApJL, 664, L79
Winter, L. M., et al., 2009, X-Ray Spectral Properties of the BAT AGN Sample, ApJ, 690, 1322
Wright, E. L., et al., 2010, The Wide-field Infrared Survey Explorer (WISE): Mission Description and Initial On-orbit Performance, AJ, 140, 1868